Banana-Shaped Mesogens Derived from 2,7-Dihydroxynaphthalene and 1,3-Dihydroxybenzene: Novel Columnar Mesophases

R. Amaranatha Reddy, B. K. Sadashiva,* and V. A. Raghunathan

Raman Research Institute, C.V. Raman Avenue, Sadashivanagar, Bangalore 560 080, India

Received April 1, 2004. Revised Manuscript Received August 5, 2004

The synthesis and mesomorphic properties of a number of compounds belonging to different homologous series and derived from 2,7-dihydroxynaphthalene are described. In addition, several compounds derived from 1,3-dihydroxybenzene have also been synthesized for comparison. All these compounds are relatively stable esters of *E-p-n*-alkoxycinnamic acids and *E-p-n*-alkoxy-α-methylcinnamic acids which are incorporated in the arms of these bent-core compounds. Many of these compounds show interesting mesophases including a novel antiferroelectric columnar phase with a rectangular lattice. Direct transitions from a rectangular columnar B_1 phase, an antiferroelectric B_2 phase, and an intercalated B_6 phase to a nematic phase have also been obtained. In addition, a direct transition from a novel columnar phase with an oblique lattice to a nematic phase has also been observed for the first time. The X-ray diffraction pattern of an oriented sample of the mesophase with an oblique lattice exhibited by a bent-core material has been reported for the first time. The possibility of a mesophase with a pseudo hexagonal lattice has also been demonstrated in bent-core compounds. The nematic phase has been obtained exclusively in compounds derived from 2,7-dihydroxynaphthalene. The influence of the central core as well as that of a fluorine substituent on the phenyl rings in the sidearms of these bent-core compounds has also been examined. The mesophases have been characterized using conventional techniques.

Introduction

Liquid crystalline phases of compounds composed of bent-core (BC) or banana-shaped molecules have evoked considerable interest during the last couple of years.[1−9] The design and synthesis of novel achiral banana-shaped mesogens forming ferro- and/or antiferro-electric smectic or columnar mesophases is one of the most exciting research activities in the area of thermotropic liquid crystals. Banana-shaped mesogens broadly require two units: (i) a central unit, which provides the bending angle, and (ii) two rodlike units with a terminal aliphatic chain which could be attached to the central unit. Although eight different Banana (B) phases have been identified and the symbols B_1 to B_8 have been

assigned for these phases by the Halle group, the B_3 and B_4 phases have now been characterized as crystals. However, the Boulder group has used a classical type nomenclature which explains more about the phase structures. As discussed,[2] the molecules of adjacent layers can have either *synclinic* (S) or *anticlinic* (A) tilted organization which is indicated by a phase symbol SmCP with subscripts "S" and "A" for C. The polar order (P) in the adjacent layers is specified by subscript "A" for antiferroelectric and "F" for ferroelectric phases, which lead to notations such as SmC_SP_A, SmC_AP_A, SmC_SP_F, and SmC_AP_F for a B_2 phase. Among these, SmC_AP_A and SmC_SP_F structures are homo chiral, while SmC_SP_A and SmC_AP_F structures are racemic. Similarly, the abbreviation "Col" has been used[7] to indicate the columnar phases and the suffixes "r" and "ob" correspond to rectangular and oblique lattices, respectively. One of the most well utilized central units has been 1,3-dihydroxybenzene or resorcinol[1−6,10−12] and its substituted derivatives.[3,9,13−15] Most of the BC compounds

* To whom correspondence should be addressed. E-mail: sadashiv@ rri.res.in.

(1) Niori, T.; Sekine, T.; Watanabe, J.; Furukawa, T.; Takezoe, H. *J. Mater. Chem.* **1996,** *6,* 1231.

(2) Link, D. R.; Natale, G.; Shao, R.; Maclennan, J. E.; Clark, N. A.; Körblova, E.; Walba, D. M. *Science* **1997,** *278,* 1924.

(3) Pelzl, G.; Diele, S.; Weissflog, W. *Adv. Mater.* **1999,** *11,* 707.

(4) Walba, D. M.; Korblova, E.; Shao, R.; Maclennan, J. E.; Link, D. R.; Glaser, M. A.; Clark, N. A. *Science* **2000,** *288,* 2181.

(5) Pratibha, R.; Madhusudana, N. V.; Sadashiva, B. K. *Science* **2000,** *288,* 2184.

(6) Sadashiva, B. K.; Raghunathan, V. A.; Pratibha, R. *Ferroelectrics* **2000,** *243,* 29.

(7) Shen, D.; Pegenau, A.; Diele, S.; Wirth, I.; Tschierske, C. *J. Am. Chem. Soc.* **2000,** *122,* 1593.

(8) Bedel, J. P.; Rouillon, J. C.; Marcerou, J. P.; Laguerre, M.; Nguyen, H. T.; Achard, M. F. *J. Mater. Chem.* **2002,** *12,* 2214.

(9) (a) Pelzl, G.; Eremin, A.; Diele, S.; Kresse, H.; Weissflog, W.; *J. Mater. Chem.* **2002,** *12,* 1316. (b) Nadasi, H.; Weissflog, W.; Eremin, A.; Pelzl, G.; Diele, S.; Das, B.; Grande, S. *J. Mater. Chem.* **2002,** *12,* 1316.

(10) Shen, D.; Diele, S.; Pelzl, G.; Wirth, I.; Tschierske, C. *J. Mater. Chem.* **1999,** *9,* 661.

(11) Amaranatha Reddy, R.; Sadashiva, B. K. *Liq. Cryst.* **2003,** *30,* 1031.

(12) Shreenivasa Murthy, H. N.; Sadashiva, B. K. *Liq. Cryst.* **2002,** *29,* 1223.

(13) Wirth, I.; Diele, S.; Eremin, A.; Pelzl, G.; Grande, S.; Kovalenko, L.; Pancenko, N.; Weissflog, W. *J. Mater. Chem.* **2001,** *11,* 1642.

(14) Amaranatha Reddy, R.; Sadashiva, B. K. *Liq. Cryst.* **2003,** *30,* 273.

(15) Shreenivasa Murthy, H. N.; Sadashiva, B. K. *Liq. Cryst.* **2003,** *30,* 1051. Shreenivasa Murthy, H. N.; Sadashiva, B. K. *J. Mater. Chem.* **2003,** *13,* 2863.

Scheme 1. General Synthetic Pathway Used for the Preparation of Bent-Core Mesogens Derived from 1,3-Dihydroxybenzene or 2,7-Dihydroxynaphthalene.
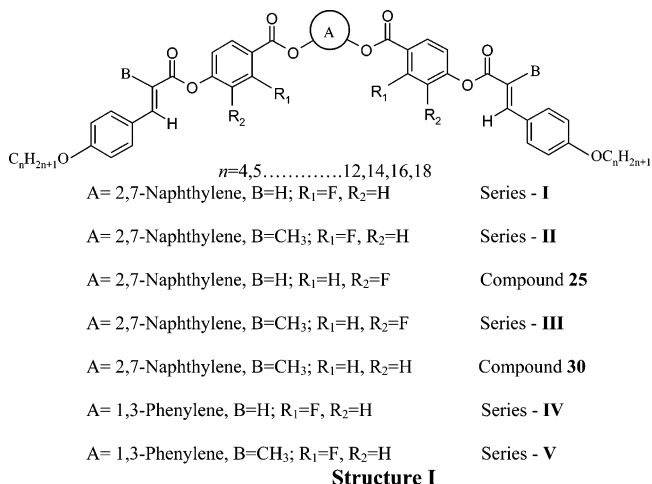

n=4,5,6........12, 14, 16,18
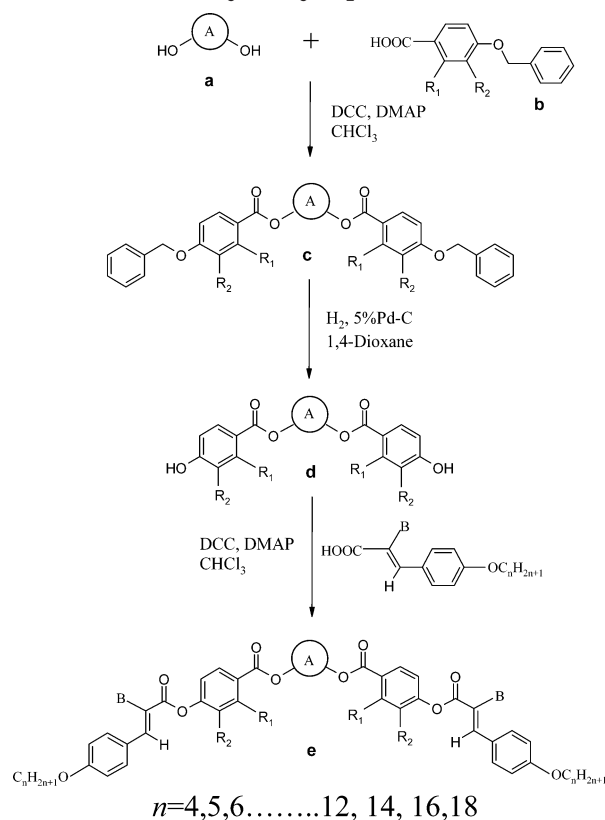
derived from these contain Schiff's base linking group in the sidearms. In addition to these, 2,7-dihydroxynaphthalene has also been used as a central unit, which provided some very interesting phases[16−18] and a new phase sequence.[17]

Most of the bent-core mesogens reported so far are monomorphic and many of them exhibit an antiferroelectric switching behavior. In addition, depending on the molecular structure of these compounds, smectic A, smectic C, or nematic phases have been obtained either individually or in combination with B-phases.[13] A direct transition from an antiferroelectric B_2 phase to a nematic phase[17,19,20] and a columnar B_1 phase to a nematic phase[10,16] have also been observed. Recently, Pelzl et al.[9a] have observed the spontaneous chiral ordering of molecules in the nematic phase. On application of an electric field to this texture, a fan-shaped texture with equidistant stripes (chiral nature) can be induced which is very unusual. Although the nematic phase has been observed in many bent-core compounds, its occurrence in combination with B-phases is very limited. Hence, there is a need to synthesize more compounds with varying molecular structure in order
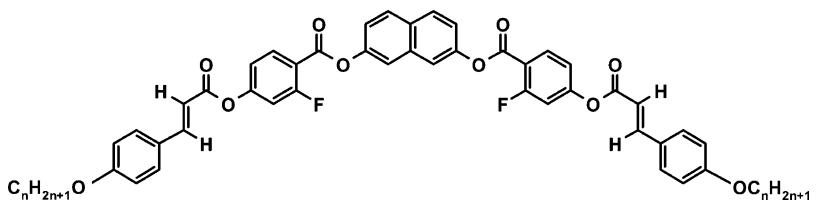
(16) Amaranatha Reddy, R.; Sadashiva, B. K. *Liq. Cryst.* **2000**, *27*, 1613.

(17) Amaranatha Reddy, R.; Sadashiva, B. K.; Dhara, S. *Chem. Commun.* **2001**, 1972.

(18) Thisayukta, J.; Nakayama, Y.; Kawauchi, S.; Takezoe, H.; Watanabe, J. *J. Am. Chem. Soc.* **2000**, *122*, 7441.

(19) Weissflog, W.; Nadasi, H.; Dunemann, U.; Pelzl, G.; Diele, S.; Eremin, A.; Kresse, H. *J. Mater. Chem.* **2001**, *11*, 2748.

(20) Schroder, M. W.; Diele, S.; Pelzl, G.; Dunemann, U.; Kresse, H.; Weissflog, W. *J. Mater. Chem.* **2003**, *13*, 1877.

to have a clear understanding of the occurrence of this type of transition. In general, the relationship between molecular structure and the mesomorphic behavior involves different aspects; for example, the position and magnitude of the bending angle, the number of phenyl rings present in the bent-core, the type and influence of lateral substituents, the nature and orientation of linking groups, and length of the terminal chains.

In this paper, we examine some novel series of bent-core compounds containing 2,7-naphthylene or 1,3-phenylene as the central unit with the side wings containing a cinnamoyloxy or an α-methylcinnamoyloxy group. The influence of the central unit and the effect of α-methyl group as well as the position of fluorine substituent in the arms have also been investigated in detail. The general molecular structure representing the different homologous series investigated is shown in structure **I**. All these bent-core compounds were prepared using a general synthetic pathway as shown in Scheme 1.

n=4,5.............12,14,16,18

A= 2,7-Naphthylene, B=H; R_1=F, R_2=H	Series - **I**
A= 2,7-Naphthylene, B=CH₃; R_1=F, R_2=H	Series - **II**
A= 2,7-Naphthylene, B=H; R_1=H, R_2=F	Compound **25**
A= 2,7-Naphthylene, B=CH₃; R_1=H, R_2=F	Series - **III**
A= 2,7-Naphthylene, B=CH₃; R_1=H, R_2=H	Compound **30**
A= 1,3-Phenylene, B=H; R_1=F, R_2=H	Series - **IV**
A= 1,3-Phenylene, B=CH₃; R_1=F, R_2=H	Series - **V**

Structure I

Results and Discussion

The phase-transition temperatures and the associated enthalpy values for the different homologous series of bent-core compounds synthesized viz. series **I**, **II**, **III**, **IV**, and **V** are summarized in Tables 1, 3, 5, 6, and 7, respectively. A total of 38 compounds were synthesized and characterized, and the appropriate mesophases were investigated. Among these, 3 are nonmesomorphic, 2 are trimorphic, 23 are dimorphic, and the remaining exhibit monomorphism.

A. Mesomorphic Properties of Compounds of Series I. As can be seen in Table 1, five enantiotropic mesophases have been obtained by the variation of *n*-alkoxy chain length. Among these, four are B-phases and the other is a nematic phase.

The lower homologues, namely compounds **1** and **2**, show two banana phases in addition to the nematic phase. Compound **2** shows the following textural features under a polarizing microscope. On cooling the isotropic liquid, the nematic phase develops in which ±1 as well as ±¹/₂ strength defects could be seen, which is an evidence for the uniaxiality of the phase. On further cooling to a temperature of about 188 °C, colorful batonnets grow and immediately transform to a focal-conic texture. This mesophase could never be aligned homeotropically, thus the possibility of a SmA phase as

Table 1. Transition Temperatures (T/°C) and Enthalpies (ΔH/kJ mol^{-1}, in Italics) for Compounds of Series I[a]

compound	n	Cr		B_{X4} (Col$_{ob^i}$)		B_{X3} (Col$_{ob}$)		B_1 (Col$_r$)		B_6 (Sm$_{intercal}$)		N		I
1	5	.	175.0 *55.6*	−		−		.	178.5 *0.12*	.	203.0 *10.1*	.	225.0 *0.89*	.
2	6	.	148.5 *42.2*	−		−		.	183.5 *0.36*	.	188.0 *9.6*	.	211.0 *0.66*	.
3	7	.	135.5 *46.1*	−		−		.	174.0 *13.1*	−		.	196.0 *0.53*	.
4	8	.	136.0 *49.8*	−		−		.	162.0 *11.4*	−		.	187.5 *0.55*	.
5	9	.	124.5 *40.5*	−		.	153.5 *11.5*	−		−		.	181.0 *0.52*	.
6	10	.	122.0 *53.6*	−		.	145.0 *11.1*	−		−		.	176.0 *0.53*	.
7	11	.	126.5 *56.7*	−		.	147.0 *10.9*	−		−		.	170.5 *0.46*	.
8	12	.	126.5 *43.8*	−		.	152.0 *13.1*	−		−		.	168.5 *0.45*	.
9	14	.	125.0 *62.4*	−		.	160.5 *14.4*	−		−		.	163.5 *0.43*	.
10	16	.	121.0 *68.4*	−		.	168.5 *17.3*	−		−		−		.
11	18	.	118.5 *76.1*	.	125.0 *0.45*	.	172.5 *18.7*	−		−		−		.

[a] Key (applicable to all tables): Cr = crystalline phase; N = nematic phase; B_1 = columnar phase with a rectangular lattice (Col$_r$); B_2 = antiferroelectric switching polar smectic C phase (SmCP$_A$); B_6 = intercalated smectic banana phase (Sm$_{intercal}$); B_{X3} = novel columnar banana phase with an oblique lattice (Col$_{ob}$); B_{X4} = more ordered columnar phase with an oblique lattice (Col$_{ob^i}$); B_{X5} = novel antiferroelectric switching columnar phase with a rectangular lattice (Col$_{rAF}$). I = isotropic phase; . = phase exists; − = phase does not exist; temperature in parentheses indicate monotropic transitions.

typical for calamitic molecules can be excluded. XRD studies show this phase to be lamellar with a periodicity comparable to half the molecular length. Hence, this mesophase has been identified as a B_6 or Sm$_{intercal}$ phase. This phase-transition enthalpy value is about 10 kJ mol^{-1}. On lowering the temperature further, this mesophase transforms to a higher ordered mesophase with a small change in the focal-conic texture. This phase transition is weakly first order (about 0.4 kJ mol^{-1}). On shearing the coverslip, this mesophase displays a mosaic texture which is the typical feature of a B_1 (Col$_r$) phase. This is consistent with the results of XRD studies, which show the presence of a two-dimensional centered rectangular lattice with the lattice parameter (b) comparable to the molecular length. The textural change accompanying the phase transition on lowering the temperature from N to B_6 is shown in Figure 1a and the textures of B_6 and B_1 phases are shown in Figure 1b and c respectively. Perhaps these represent the first example of compounds showing a direct transition from the nematic phase to a B_6 phase and a phase sequence of N to B_6 to B_1. The XRD pattern of an oriented sample suggests the orthogonal alignment of bent-core molecules in both B_6 and B_1 mesophases (see compounds **12**−**16** for more details). It should be noted that the birefringent textures under a polarizing microscope for B_6 and B_1 phases could be due to intercalated structures which restrict the rotation around the long axes of the molecules. On increasing the terminal chain length, the core−core and the chain−chain interactions increase and hence a few BC mol-

ecules join together to form clusters. These clusters arrange themselves in an antiferroelectric order to form a lattice such that they stabilize the columnar phase and hence a direct transition from N to B_1 phase is observed for compounds **3** and **4**. Interestingly, the direct transitions from N to B_6 and N to B_1 phases could be obtained on ascending the homologous series. As shown in Figure 2, the spacings of the (11) and (02) reflections in the B_1 phase increase on ascending the homologous series, with the former rising faster. They cross over at compound **3**. Hence, the reflections from this system can be indexed on a hexagonal lattice. However, this is due to the fact that the lattice parameter b is almost equal to $\sqrt{3}\ a$, and this phase is not truly hexagonal. Both the lattice parameters a and b increase within the series; the increase in b reflects the increase in the molecular length and the increase in a indicates an increase in the number of molecules in a lattice.

The textures obtained for the higher homologues (compounds **5**−**11**) are somewhat similar to a columnar B_1 phase but distinguishable features could be clearly seen. On cooling the nematic phase of compound **9**, a flowerlike pattern develops as shown in Figure 3a and this transforms to an undefined texture on lowering the temperature. A growth of small mosaic-like pattern could also be seen. Compound **10** exhibits spherulitic growth pattern in addition to the more complex textural pattern as shown in Figure 3b and c. As can be seen in Figure 3b, the extinction (dark brushes) obtained in
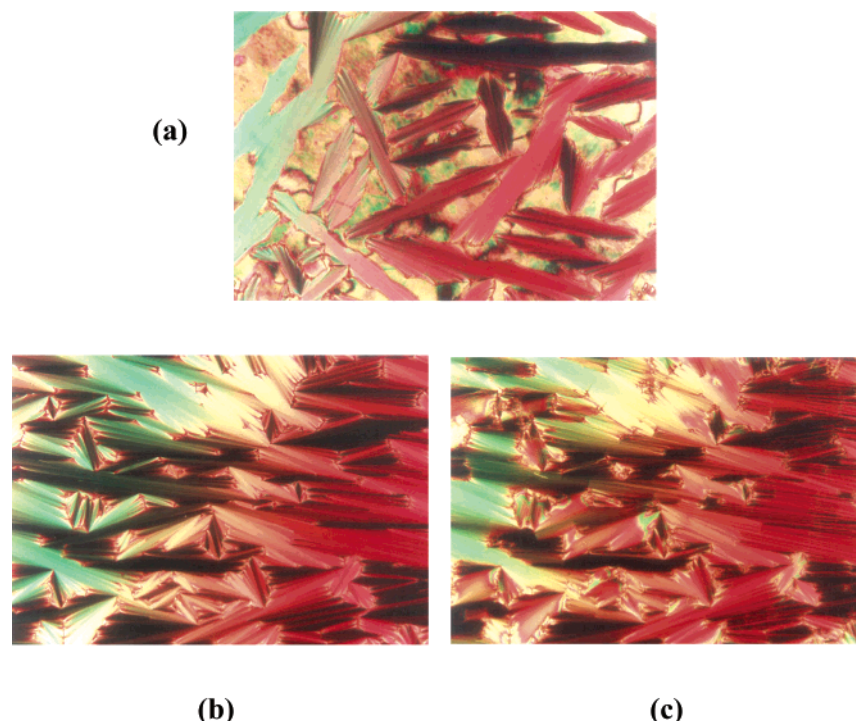
Figure 1. Optical photomicrographs obtained for compound **2**: (a) B_6 phase developing from the nematic phase; (b) completely formed B_6 phase at 184 °C; and (c) B_1 phase after transition at 175 °C, same region as in (b).
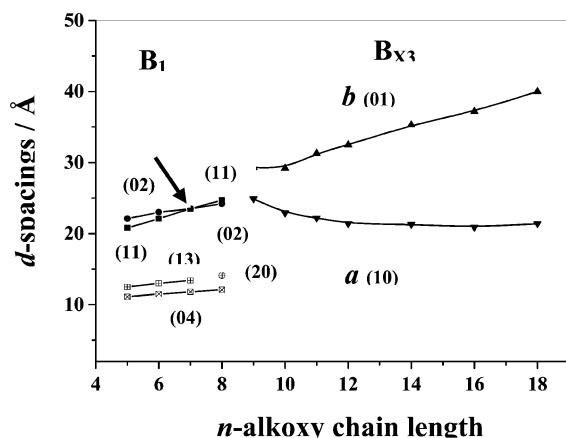

Figure 2. Plot of *d*-spacings obtained in the B_1 mesophase and the lattice parameter values *a* and *b* for the B_{X3} mesophase as a function of *n*-alkoxy chain length for the compounds of series **I**. The arrow shows the homologue at which the spacings of the (11) and (02) planes cross in the B_1 phase (pseudo hexagonal lattice) on ascending the series.

some circular domains makes an angle wrt the directions of the crossed polarizers indicating a synclinic tilt of the molecules in adjacent columns. This mesophase has been designated as a B_{X3} (Col_{ob}) mesophase. The symbols B_{X1} and B_{X2} have already been used by us to designate smectic and two-dimensional ferroelectric phases, respectively.[21]

Oriented X-ray diffraction patterns have been obtained for most of the compounds exhibiting B_{X3} mesophase and the data are summarized in Table 2. All these compounds show diffuse wide-angle reflections in this phase, showing the absence of any long-range in-plane positional order. The reflections in the small angle

(21) Amaranatha Reddy, R.; Sadashiva, B. K. *J. Mater. Chem.* **2002**, *12*, 2627.

region cannot be indexed on a rectangular lattice with the indexing scheme used in the case of the B_1 phase. We also tried other possible schemes, but were unable to fit them to a rectangular lattice. However, the oriented XRD patterns obtained from an aligned sample indicated the presence of an oblique lattice. Based on these, observed and calculated Miller indices as well as the lattice parameter values obtained are recorded in Table 2. The X-ray diffraction patterns of oriented samples obtained in the B_{X3} phase of compounds **6** and **8** are shown in Figure 4a and b, respectively. As can be seen in Figure 4a and b, the outer diffuse scattering maxima are located out of the equator, which indicates a tilt of the molecules within the oblique lattice. The lattice parameter values *a* and *b* obtained for this mesophase were plotted as a function of chain length and are shown in Figure 2. It is interesting to note that the oblique angle β varies for the B_{X3} mesophase on ascending the homologous series. It is 72.3° for compound **5** and becomes almost rectangular ($\beta = 91$) for compound **7** which decreases to 84.4° for compound **11** on ascending the homologous series. The B_{X3} to isotropic phase-transition enthalpy value is not very high and varies from 11 to 19 kJ mol^{-1}. No electrooptical current response could be observed in the B_{X3} mesophase even at electric fields of about ±30 V/μm.

Compound **11** shows an additional mesophase which appears at a lower temperature wrt the B_{X3} (Col_{ob}) phase and has been designated as B_{X4} (Col_{ob}^1). The phase transition takes place to the B_{X4} phase with additional sharp lines over the fan-shaped pattern of the B_{X3} phase. The phase-transition enthalpy is about 0.4 kJ mol^{-1}. The optical textures observed in the B_{X3} and the B_{X4} phases are shown in Figure S1 in the Supporting Information. The X-ray diffraction data from the B_{X4} phase of compound **11** can also be indexed on an oblique lattice as shown in Table 2. Moreover, no
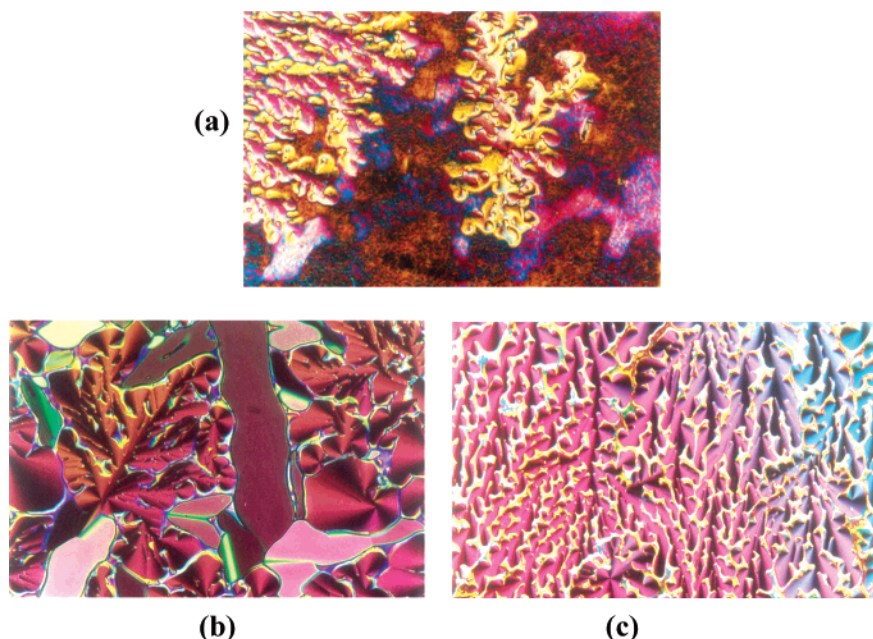
Figure 3. Optical photomicrographs of (a) flowerlike pattern of the B_{X3} phase growing from the nematic phase of compound **9**; (b) tiny mosaics and spherulitic growth pattern obtained in the B_{X3} mesophase exhibited by compound **10**; and (c) more complex textural pattern obtained in the B_{X3} mesophase of compound **10** at 152 °C.

Table 2. *d*-Spacings Obtained for Different Mesophases and the Corresponding Miller Indices for the Compounds of Homologous Series I[a]

compound	*d*-spacings (Å) (Miller indices)	lattice parameters (Å)		phase type	oblique angle β (deg.)
		a	*b*		
1	22.1 (01), 11.1 (02)	−	−	B_6	−
	22.1 (02), 20.8 (11), 12.5 (13), 11.1 (04)	23.6	44.2	B_1	−
2	23.0 (01), 11.5 (02)	−	−	B_6	−
	23.0 (02), 22.1 (11), 13.0 (13), 11.5 (04)	25.1	46.0	B_1	−
3	23.5 (02 & 11), 13.4 (13), 11.8 (04)	27.1	47.0	B_1	−
4	24.7 (11), 24.2 (02), 14.1 (20), 12.1 (04)	28.7	48.5	B_1	−
5	27.9 (01), 23.7 (10), 21.6 (11), 16.0 (1 $\bar{1}$), 14.0(12), 12.0 (21), 9.9 (2 $\bar{1}$ or 13); Calc: 15.8(1 $\bar{1}$), 14.0(12), 12.3(21), 9.9(2 $\bar{1}$), 9.7(13)	24.9	29.3	B_{X3}	72.3
6	29.1(01), 22.8 (10), 18.6(11), 14.6 (02), 12.0 (1 $\bar{2}$), 10.5(2 $\bar{1}$), 8.9(2 $\bar{1}$ or 1 $\bar{3}$); Calc:14.6 (02), 11.9 (1 $\bar{2}$), 10.4(2 $\bar{1}$), 8.7 (2 $\bar{2}$), 8.7 (1 $\bar{3}$)	22.9	29.2	B_{X3}	86
7	31.3(01), 22.2(10), 18.0 (11), 15.9 (02), 12.8 (1 $\bar{2}$ or 12), 10.7(03 or 2 $\bar{1}$ or 21), 9.2 (2 $\bar{2}$ or 13); Calc: 15.7(02), 12.9(1 $\bar{2}$), 12.7(12), 10.4(03), 10.5(2 $\bar{1}$), 10.4 (21), 9.1 (2 $\bar{2}$), 9.4(13).	22.2	31.3	B_{X3}	91
8	32.5 (01), 21.4(10), 17.6 (11), 16.3 (02), 13.4(1 $\bar{2}$), 12.7(12), 10.9 (03), 10.5(2 $\bar{1}$), 9.2(2 $\bar{2}$); Calc: 16.3(02), 13.2(1 $\bar{2}$), 12.7(12), 10.8(03), 10.3(2 $\bar{1}$), 9.1(2 $\bar{2}$).	21.4	32.5	B_{X3}	92
9	35.2 (01), 21.2 (10), 17.6 (11 & 02), 14.1 (1 $\bar{2}$), 13.0(12), 11.7 (03); Calc: 17.6(02), 14.1(1 $\bar{2}$), 13.1(12), 11.7 (03)	21.3	35.3	B_{X3}	94.3
10	37.1(01), 20.9 (10), 18.6(02), 17.6 (11), 14.8 (1 $\bar{2}$), 13.3(12), 12.4(03); Calc:18.6 (02), 14.5 (1 $\bar{2}$), 13.3(12), 12.3(03)	20.9	37.2	B_{X3}	86.6
11	39.8(01), 21.3(10), 19.9 (02), 19.6 (11), 17.9 (1 $\bar{1}$), 13.8(1 $\bar{2}$), 13.2 (03), 9.4(14); Calc: 19.9(02), 18.1(1 $\bar{1}$), 13.9(1 $\bar{2}$), 13.3(03), 9.4(14).	21.4	40.0	B_{X3}	84.4
11	39.3(01), 20.9(10), 19.7 (02), 17.8 (1 $\bar{1}$), 15.2(12), 13.0(03), 10.7 (1 $\bar{3}$), 10.0(2 $\bar{1}$); Calc:14.9(12), 13.1(03), 10.6 (1 $\bar{3}$), 9.8(2 $\bar{1}$)	20.8	39.1	B_{X4}	84.8

[a] XRD measurements have been carried out on mesophases obtained on cooling.

polarization current peak /s were observed up to about ± 40 V/μm in both the B_{X3} and B_{X4} phases.

Figure 5 shows a plot of the transition temperatures as a function of *n*-alkoxy chain length for the compounds of series **I**. The clearing temperature curves obtained for N and B_6 phases fall steeply while the curve obtained for the B_1 phase rises initially and then falls on ascending the homologous series. However, the clearing temperature curve obtained for B_{X3} phase falls initially and then rises gradually on ascending the homologous series and all the points fall on a smooth curve. Interestingly, the nematic phase exists even for the

higher homologues, up to the *n*-tetradecyloxy derivative which is rather unusual for compounds exhibiting banana phases. As we shall see later, even by shifting the fluorine substituent in the middle phenyl ring from *ortho* to *meta* position, similar phase behavior could be observed (compound **25**) without significant change in the transition temperatures.

It is interesting to note that the lower homologues show a B_1 phase with a rectangular lattice while the higher homologues show a columnar phase with an oblique lattice. Thus, the direct transitions from N to B_1 (Col_r) and N to B_{X3} (Col_{ob}) phases have been obtained
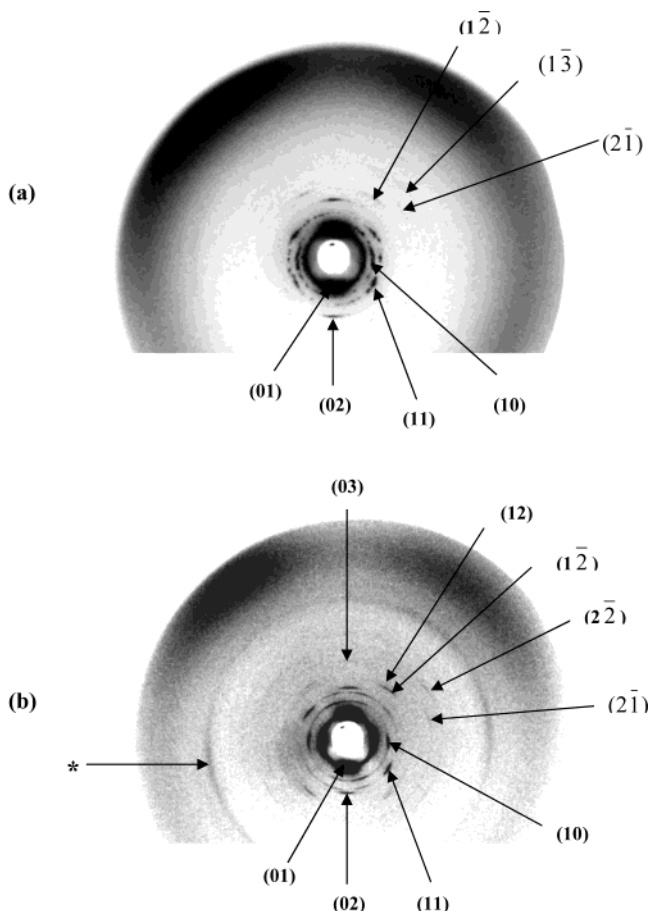
Figure 4. Oriented X-ray diffraction patterns obtained in the B_{X3} mesophase for (a) compound **6** at 130 °C and (b) compound **8** at 135 °C. (*): reflection is due to the Mylar windows of the sample chamber.
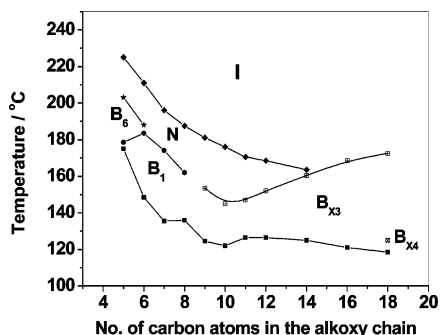

Figure 5. Plot of transition temperatures as a function of *n*-alkoxy chain length obtained for the compounds of series **I**.

on ascending the homologous series. For further investigation, miscibility studies were carried out between B_1 and B_{X3} mesophases and complete miscibility could not be obtained. These investigations suggest that the organization of molecules in these two mesophases is different. As observed from X-ray investigations, B_1 phase with short chain compounds (**1−4**) shows the orthogonal arrangement of molecules and the long chain compounds (**9−18**) induce a tilt of molecules. We believe that in both the cases the polarization vector is perpendicular to the plane formed by the 2D modulation. The orthogonal arrangement for short chains maintains a rectangular lattice and especially the synclinic tilt of molecules for long chains deviate and the lattice becomes oblique. Furthermore, decrease in the value of

lattice parameter *b* (see Table 2) for the successive homologues between the two lattices is clearly an evidence for the tilt of the molecules. In fact, very recently Szydlowska et al.[22] have described two columnar phases of bent-core molecules with a two-dimensional structure modulated in the plane perpendicular to the direction of the spontaneous polarization vector. They also speculated that the molecules with twisted banana branches wrt the plane of the central phenyl ring would prefer to stack along the polar axis. In the presently investigated series of compounds, this is possible due to the presence of flexible cinnamoyl groups in the wings.

B. Mesomorphic Properties of Compounds of Series II and III. An examination of compound **13** of series **II** under a polarizing microscope reveals the following features. On cooling the isotropic liquid, a uniaxial nematic phase appears as indicated by the observation of 2- and 4-brush defects. On cooling the nematic phase, a mosaic texture that is normally observed for a B_1 phase appears, and a photomicrograph of this is shown in Figure S2. The X-ray diffractogram of an unoriented sample of compound **13** obtained is shown in Figure 6a. The wide-angle diffuse peak at around 4.7 Å indicates a liquidlike in-plane order. The three peaks in the small angle region, with their spacings in the ratio $1:1/\sqrt{3}:1/2$ are suggestive of a hexagonal lattice. However, as in the case of compound **3**, they can also arise from a centered rectangular lattice, when the two lattice parameters are related by $b = \sqrt{3}\ a$. To check this possibility we have collected the diffraction pattern (see Figure 6b) of an oriented sample of compound **13**. As can be seen, a hexagonal symmetry can be ruled out from the preferred orientation of the wide-angle chain reflections. Hence, this phase can be identified as B_1 phase with a rectangular centered lattice (Col$_r$). The relative orientation of the wide-angle reflections with respect to the small angle ones indicates the orthogonal arrangement of the molecules in this phase as described by Pelz et al.[23] for their compounds.

On ascending the homologous series, compounds **14−17** show textural patterns similar to those of a B_1 phase, and the X-ray data obtained can be indexed for a rectangular unit cell having an orthogonal alignment of the molecules as shown in Table 4. The X-ray diffractogram obtained in the B_1 phase exhibited by compound **16** is shown in Figure S3. It is interesting to note that the lattice parameter value *b* (layer thickness) is comparable for the same chain lengths between the two series (**I** and **II**) of compounds (**1−4** and **13−16**) exhibiting the orthogonal B_1 phase. On ascending the homologous series the B_1 phase obtained for homologues with shorter chain lengths gets eliminated. For example, compound **18** exhibits only a nematic phase.

The higher homologues, namely compounds **19−22**, show a banana phase along with the nematic phase. For example, on cooling the isotropic liquid of compound **21**, a nematic phase with a schlieren texture was obtained and a photomicrograph of this is shown in Figure S4.

(22) Szydlowska, J.; Mieczkowski, J.; Matraszek, J.; Bruce, D. W.; Gorecka, E.; Pociecha, D.; Guillon, D. *Phys. Rev. E* **2003**, *67*, 31702.
(23) Pelz, K.; Weissflog, W.; Baumeister, U.; Diele, S. *Liq. Cryst.* **2003**, *30*, 1151.
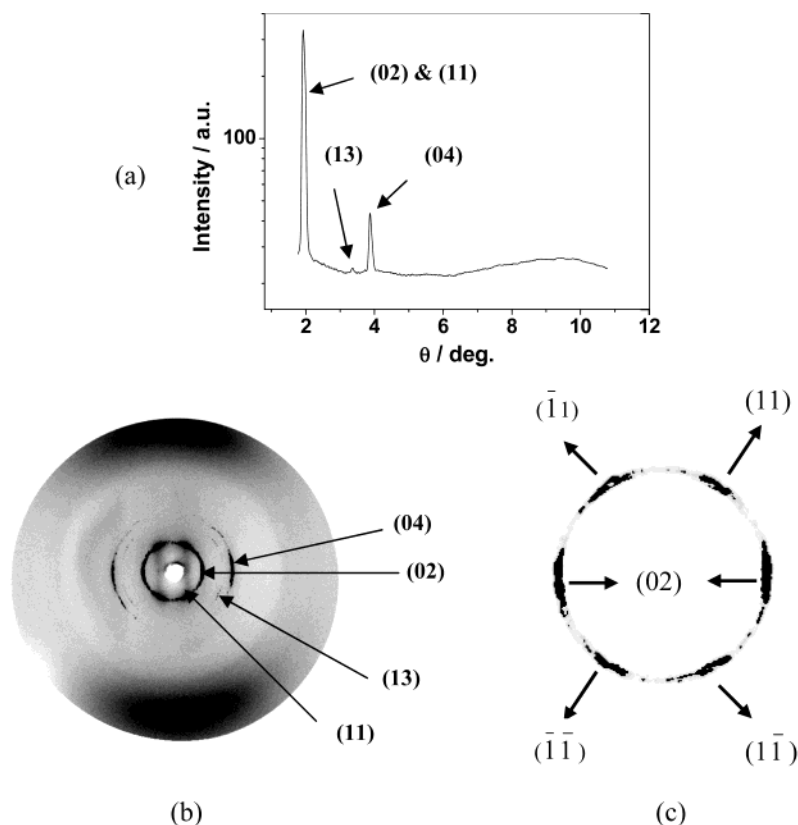
Figure 6. (a) X-ray diffractogram obtained for compound **13** in the B_1 mesophase at 134 °C. (b) Oriented X-ray diffraction pattern obtained in the B_1 mesophase of compound **13** indicating the orthogonal arrangement of the molecules in a rectangular lattice. (c) Strong small angle reflections in (b) showing a pseudo 6-fold symmetry due to the specific relation between the lattice parameters *a* and *b*, as discussed in the text.

However, on very slow cooling, the nematic phase appeared with 2- and 4-brush defects indicating the uniaxial character of the phase. On further slow cooling, fingerprint texture developed from the nematic phase and the whole field of view was filled completely with this texture. This textural feature is indicative of a lamellar B_2 (SmCP$_A$) phase. The transition enthalpy value obtained for this mesophase is in the range of $12-14$ kJ mol^{-1} which is normally obtained for a B_2 phase. However, the nematic phase obtained could never be aligned homeotropically even in cells treated for such an alignment. In contrast, this aligns very well in cells treated for homogeneous alignment.[17] On ascending the homologous series, the nematic phase gets eliminated and only the B_2 phase is stabilized as observed for compounds **23** and **24**. The X-ray diffraction pattern obtained for the lower temperature mesophase of un-oriented samples of compounds **21** and **22** and meso-phase of compound **23** show lamellar reflections in the small angle region and a diffuse peak in the wide-angle region at about 4.6 Å, indicating the absence of in-plane order. The calculated tilt angle is about 46°.
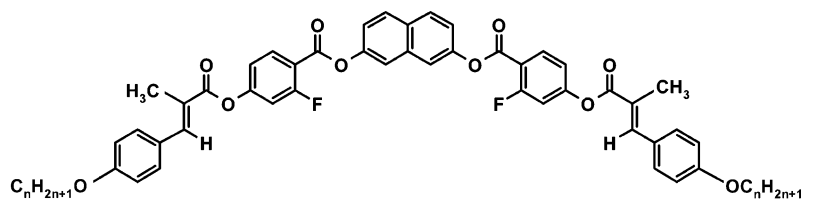
A plot of the *d*-spacings as a function of the terminal chain length obtained for this homologous series is shown in Figure 7. As can be seen, for a B_1 phase, the *d*-values of (02) and (11) increase on ascending the homologous series. The difference between the *d*-values of (02) and (11) decreases on lowering the number of carbon atoms in the *n*-alkoxy chain and hence these two are overlapping for compounds **12** and **13** (see Figure 6b and c). The layer spacing for the compounds of B_2

phase gradually increases on ascending the homologous series.

A plot of the transition temperatures as a function of *n*-alkoxy chain length obtained for the compounds of homologous series **II** is shown in Figure S5. The N−I phase transition temperatures gradually decrease on increasing the chain length. The B_1−I phase transition temperature curve falls steeply while the clearing temperature points for the B_2 phase rises initially and lie on a smooth curve on ascending the homologous series.

By changing the position of the fluorine substituent in the middle phenyl ring from *ortho* to *meta* position (series **III**), the mesomorphic behavior is retained with marginal changes in the transition temperatures. As can be seen in Table 5, compound **26** shows a columnar B_1 phase in addition to a nematic phase. The next two higher homologues, namely compounds **27** and **28**, show a lamellar B_2 phase and a nematic phase. On cooling the nematic phase of compounds **26** and **28** transition takes place to B_1 and a B_2 phases, respectively. However, compound **29** shows only the antiferroelectric B_2 phase. The optical photomicrographs obtained for I−N, N−B_1, and N−B_2 phases are shown in Figure 8 a, b, and c, respectively.

For the compounds of series **III**, the XRD studies confirmed the existence of a rectangular lattice in the B_1 phase and lamellar ordering in the B_2 phase. As can be seen, independent of the position of fluorine in the middle phenyl ring, the nematic phase gets stabilized even for compounds with long chain lengths.

Table 3. Transition Temperatures (*T*/°C) and Enthalpies (Δ*H*/kJ mol⁻¹, in Italics) for Compounds of Series II[a]

compound	*n*	Cr		B₂ (SmCP$_A$)		B₁ (Col$_r$)		N		I	ref
12	4	.	143.5	−		.	(140.5)	.	184.0	.	
			44.8				*10.6*		*0.75*		
13	5	.	133.0	−		.	138.0	.	164.0	.	
			31.3				*10.4*		*0.57*		
14	6	.	128.5	−		.	134.0	.	159.0	.	
			38.3				*9.7*		*0.53*		
15	7	.	133.5	−		.	(126.5)	.	148.5	.	
			72.1				*11.8*		*0.55*		
16	8	.	121.5	−		.	(118.5)	.	145.0	.	
			62.2				*11.0*		*0.45*		
17	9	.	118.0	−		.	(109.5)	.	137.0	.	
			60.1				*9.9*		*0.43*		
18	10	.	116.5	−		−		.	134.0	.	
			63.4						*0.46*		
19	11	.	111.5[b]	.	(110.5)[c]	−		.	130.5	.	
			101.2		*12.3*				*0.49*		
20	12	.	119.5	.	(116.0)	−		.	127.0	.	17
			75.6		*13.2*				*0.49*		
21	13	.	117.5	.	120.0	−		.	125.0	.	17
			59.3		*13.9*				*0.43*		
22	14	.	107.0	.	123.0	−		.	124.0	.	17
			58.6		*14.1*				*0.34*		
23	16	.	108.0	.	128.0	−		−		.	17
			52.4		*16.8*						
24	18	.	109.0[b]	.	132.0	−		−		.	
			115.3		*15.9*						

[a] Same as footnote *a* for Table 1. [b] Compound has crystal−crystal transition; enthalpy denoted is the sum of all previous transitions. [c] Temperature obtained on cooling.

Table 4. *d*-Spacings Obtained for Different Mesophases and the Corresponding Miller Indices for the Compounds of Homologous Series II

compound	*d*-spacings (Å)/(Miller indices)	lattice parameters /Å		phase type	*T*/°C
		a	*b*		
12	21.3(02)&(11), 12.3(13), 10.7(04)	24.6	42.6	B₁	137
13	22.1(02)&(11), 12.9(13), 11.0(04)	25.5	44.2	B₁	135
14	24.0 (11), 22.9 (02), 13.4 (13), 11.5 (04)	28.2	45.8	B₁	130
15	25.3 (11), 23.5 (02), 14.0 (13), 11.8 (04)	30.0	47.0	B₁	124
16	26.3 (11), 24.2 (02), 12.3 (04)	31.2	48.4	B₁	116
21	39.2 (01), 19.7 (02)	−	39.2	B₂	117
22	40.6 (01), 20.3 (02)	−	40.6	B₂	115
23	44.3 (01), 22.5 (02), 14.9 (03)	−	44.3	B₂	120

[a] XRD measurements have been carried out on the mesophases obtained on cooling.

Compound **25**   Cr 142.0 B$_{X3}$ (Col$_{ob}$) 154.0 N 161.0 I
99.7   *12.7*   *0.5*
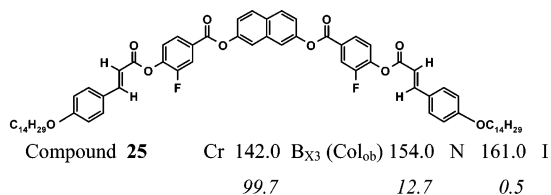
To confirm the antiferroelectric ground-state structure of the B₂ phase, a triangular-wave method was employed. In addition, dc field experiments indicated only a racemic ground-state structure in the B₂ phase. The X-ray diffractogram and the current response trace obtained for the B₂ phase exhibited by compound **28** are shown in Figure 9a and b, respectively.

In the presently investigated compounds, a wide variety of columnar as well as smectic phases could be observed below the nematic phase (see Figure 10). Observation of N to B-phases is perhaps due to a temperature-dependent bending angle which is attributed to a conformational flexibility of the cinnamoyloxy linking groups. All possible models for the B₁ phase are also indicated.

C. Mesomorphic Properties of Compounds of Series IV and Series V. As observed for the lower homologues of series **I**, compound **31** shows B₆ and B₁

Table 5. Transition Temperatures (T/°C) and Enthalpies [ΔH/kJ mol^{-1}, in Italics] for Compounds of Series III[a]

compound	n	Cr		B$_2$ (SmCP$_A$)		B$_1$ (Col$_r$)		N		I
26	12	.	111.0	—		.	112.0	.	124.0	.
			44.1				*10.2*		*0.46*	
27	13	.	112.0	.	114.0	—		.	122.5	.
			90.4		*10.5*				*0.46*	
28	14	.	102.0	.	117.0	—		.	121.8	.
			55.6		*10.9*				*0.51*	
29	16	.	107.0	.	122.5	—		—		.
			91.9		*11.7*					

Compound **30**   Cr 143.0 I
95.3

phases which were confirmed by XRD studies as described below. In the small angle region, two sharp reflections were obtained at $d_1 = 21.1$ Å and $d_2 = 10.6$ Å, and they can be assigned as (01) and (02) respectively for a B$_6$ phase. On lowering the temperature, a phase transition takes place and XRD data of this phase shows four sharp reflections in the small angle region corresponding to $d_1 = 21.1$ Å, $d_2 = 18.5$ Å, $d_3 = 12.8$ Å, and $d_4 = 10.6$ Å. They can be indexed as (11), (02), (20), and (22) respectively for a centered rectangular lattice with the lattice parameters, $a = 25.7$ Å and $b = 37$ Å and the mesophase has been identified as a B$_1$ phase.

However, the textural features observed for the higher homologues (compounds **32−36**) are completely different from the B$_6$ and B$_1$ phases. On slow cooling of a thin film of the isotropic liquid of compound **35**, an unusual complex texture was obtained and a photomicrograph of this is shown in Figure 11. Sometimes, this mesophase shows spherulites in addition to small platelike mosaics. The enthalpy value obtained for this mesophase−isotropic transition varies and is about 10 to 17 kJ mol^{-1}. This mesophase has been designated as a B$_{X5}$ (Col$_{rAF}$) phase.
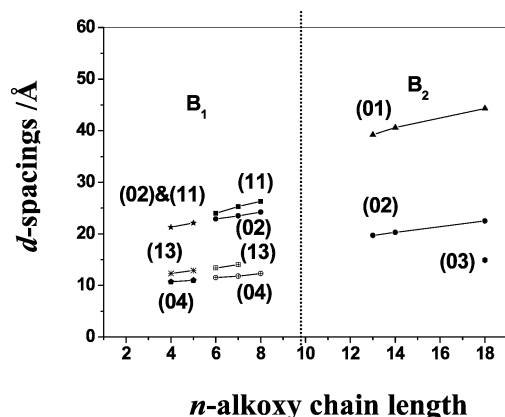
Figure 7. Plot of d-spacings as a function of n-alkoxy chain length obtained for the mesophases exhibited by compounds of series **II**.

The X-ray diffraction pattern of an oriented sample obtained for the B$_{X5}$ mesophase of compound **36** shows the following. The small angle sharp reflections obtained at $d_1 = 38.4$ Å, $d_2 = 19.3$ Å, $d_3 = 17.5$ Å, $d_4 = 14$ Å, and $d_5 = 12.9$ Å, however, could be indexed as (01), (02), (11), (12),and (03) respectively for a rectangular lattice, with lattice parameters, $a = 19.7$ Å and $b = 38.4$ Å. Compound **35** also shows five sharp reflections in the small angle region at $d_1 = 36.3$ Å, $d_2 = 18.3$ Å, $d_3 = 16.5$ Å, $d_4 = 12.7$ Å and $d_5 = 12.2$ Å. Based on the XRD data obtained from oriented samples, these could also be indexed as (01), (02), (11), (12), and (03), respectively, for a rectangular lattice, with lattice parameters $a = 18.5$ Å and $b = 36.5$ Å. The wide-angle diffuse regions obtained in both the cases show the absence of any long-range in-plane positional order with a tilted organization of molecules. The estimated number of molecules is about 3 per unit cell and is relatively low when compared with the other mesophases of a rectangular lattice.[23]

In addition, the mesophase exhibited by compounds **32−36** shows an interesting electrooptical switching behavior. For example, compound **35** shows two polarization current peaks for each half cycle on applying a triangular-wave electric field of about ±23 V/μm and at a frequency of 30 Hz (threshold voltage ±20 V/μm) at 114 °C, indicating an antiferroelectric ground state for the mesophase. The calculated spontaneous polarization value is about 350 nC cm^{-2}. The current response trace obtained in this B$_{X5}$ mesophase is shown in Figure 12. The texture also changes by the application of an electric field. On turning off the applied field, the texture relaxes in which a striped pattern is observed as shown in Figure S6. The presence of a striped pattern in the absence of electric field, as in the case of racemic B$_2$ phase, suggests that the adjacent columns have a synclinic tilt of the molecules. During the preparation of this manuscript, we came across a very recent paper by Ortega et al.[24] who have observed a clear electric field induced Col$_r$−SmCP$_A$ (B$_1$−B$_2$) phase
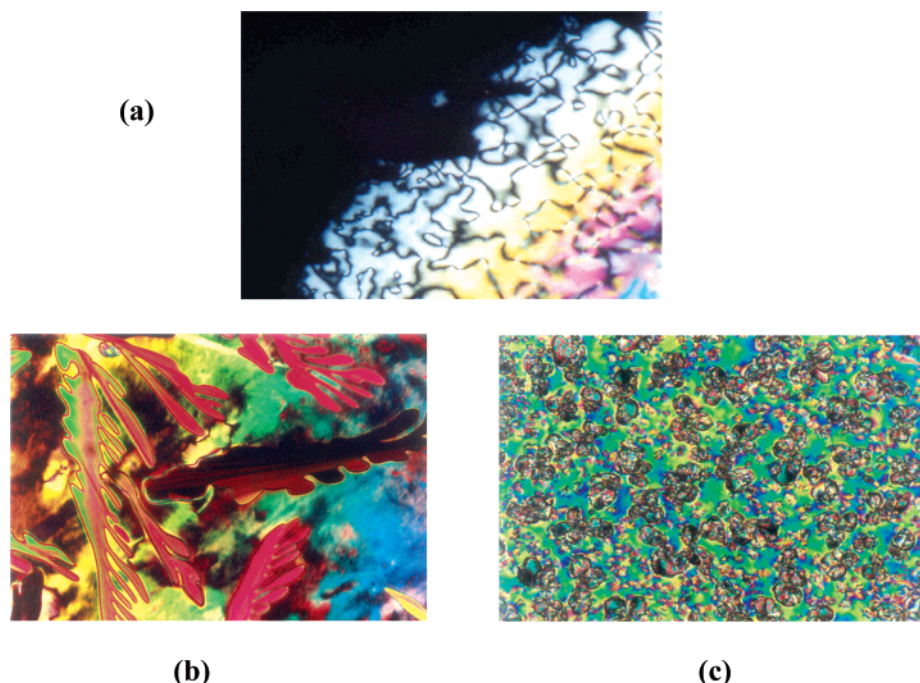
Figure 8. (a) A uniaxial nematic phase developing from the isotropic liquid of compound **26**. (b) Transition from the nematic phase to a B_1 phase obtained for compound **26**. (c) Transition from the nematic phase to a B_2 phase obtained for compound **28**.
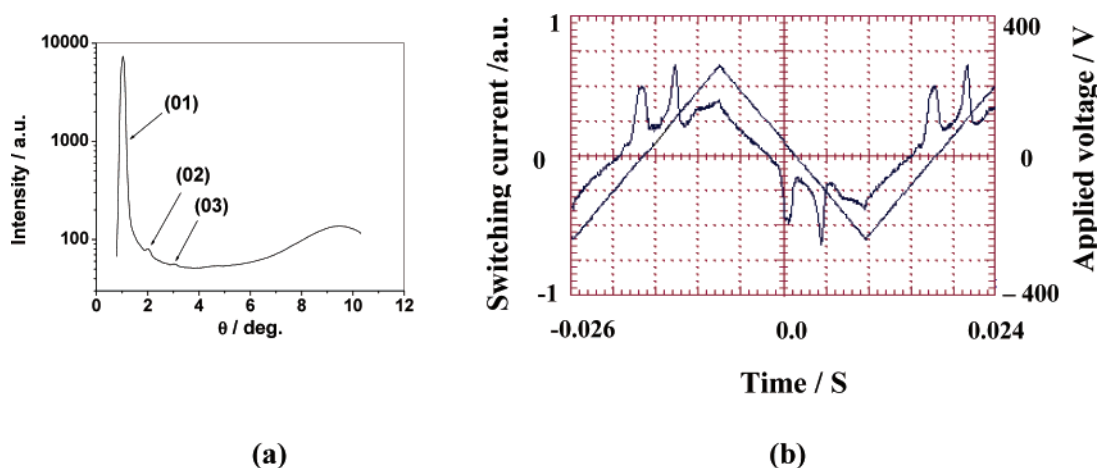

Figure 9. (a) X-ray diffractogram obtained in the B_2 mesophase of compound **28** at 110 °C and (b) the switching current response obtained for the same compound by applying a triangular voltage (±250 V, 30 Hz) at 110 °C. Sample thickness 9.6 μm; polarization, $P \approx 590$ nC cm^{-2}.

transition. Although they did not detect any switching current during the transition, a clear electrooptic effect was observed. More importantly, contrary to our observation, they observed a recovery of the columnar structure upon removal of the electric field. Based on our experimental observations, we have proposed possible models for an oblique lattice as well as a rectangular lattice in which the polar axis coincides with the column axis and is perpendicular to the plane of the 2D modulation. The polarization direction alternates either in adjacent columns or layers (antiferroelectric ordering) due to dipolar interactions, and has a synclinic tilt as shown in Figure 13. The estimated number of molecules amounts to 3 per unit cell in both oblique and rectangular lattices (B_{X3} and B_{X5} phases, respectively). This

agrees well with the proposed models shown in Figure 13 which are somewhat similar to the model recently proposed by Tschierske et al.[25] for a ferroelectric phase with an oblique lattice.

However, compounds **37** and **38** (Table 7), which contain a α-methylcinnamoyloxy group in the side wings, do not show any mesophase. The presence of a methyl group in the cinnamoyl moiety of these five-ring esters completely destroys the mesophase probably due to steric reasons.

D. Comparison Between the Mesophases of Compounds of Series I, II, and III. Compounds of series **I** exhibit 4 different B-phases, namely B_6, B_1, B_{X3}, and B_{X4}, in addition to a nematic phase. Among these, B_6 and B_1 phases show an orthogonal arrangement of molecules; and B_{X3} and B_{X4} phases show an oblique

(24) Ortega, J.; de la Fuente, M. R.; Etxebarria, J.; Folcia, C. L.; Diez, S.; Gallastegui, J. A.; Gimeno, N.; Ros, M. B.; Perez-Jubindo, M. A. *Phys. Rev. E* **2004**, *69*, 11703.

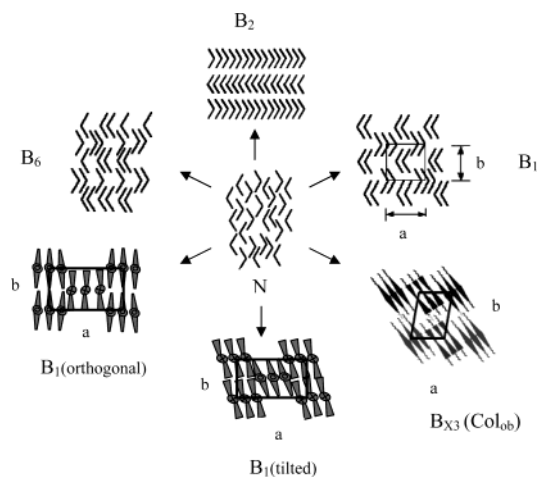(25) Tschierske, C. *Pramana-J. Phys.* **2003**, *61*, 455.

Figure 10. Observed phase transitions and possible ways to escape a macroscopic polarization in the smectic as well as columnar phases made up of bent-core molecules.
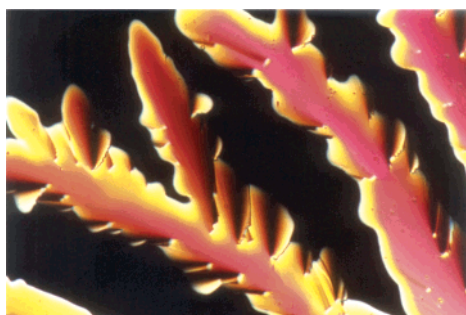

Figure 11. Unusual texture of the B_{X5} mesophase obtained on cooling the isotropic liquid of compound **35** at 118.5 °C.
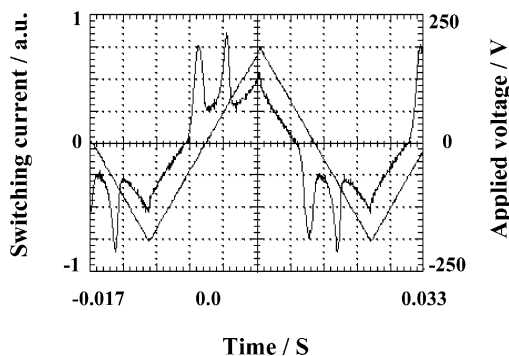

Figure 12. Switching current response obtained in the B_{X5} mesophase of compound **35** by applying a triangular voltage (±187 V, 30 Hz) at 114 °C. Sample thickness 8 μm; polarization, $P \approx 350$ nC cm^{-2}.

lattice with a tilted organization of molecules. However, no electrooptical current response could be observed in any of these phases even for long chain compounds. This could be due to a free rotation of molecules around the long axes in the columnar phases as indicated by the presence of a nematic phase at higher temperature.

In series **II**, by introducing an α-methylcinnamoyloxy moiety, the columnar oblique lattice is completely eliminated but a switchable lamellar B_2 phase is induced for the higher homologues. As expected, a reduction in transition temperatures was observed when compared to the parent cinnamoyloxy derivatives and this modification in the mesophases and temperatures can be attributed to the lateral α-methyl group (steric factors). This homologous series of compounds exhibit

a nematic, B_1, and B_2 mesophases, and interestingly B_1 phase shows the orthogonal arrangement of molecules.

The change in the position of fluorine substituent in the middle phenyl ring from *ortho* to *meta* position (compounds **9** and **25**), does not affect the mesomorphic behavior except for minor changes in the transition temperatures. However, sometimes it is very effective. For example, compound **20** shows a B_2 phase while the corresponding *meta* substituted analogue (compound **26**) exhibits a columnar B_1 phase.

Surprisingly, the unsubstituted parent compound **30** does not show any mesophase and melts at 143 °C while the corresponding fluorine substituted compounds, namely compounds **20** and **26**, show direct transitions from N to B_2 and N to B_1 phases, respectively. This is one of the best examples to show that although the parent compounds do not show any mesophase, the fluorine substitution induces both N and B-phases (B_1 and B_2 phases). This is contrary to our earlier observations[11] in which the fluorine substitution in the middle phenyl ring eliminated the existing mesophases. Though fluorine is significantly larger in size than hydrogen, the electronegative character of the former has strong influence on the occurrence as well as the type of mesophase.

E. Comparison Between the Mesophases of Compounds of Series IV and V. These bent-core compounds are derived from resorcinol, containing a fluorine at *ortho* position on the middle phenyl ring, and the arms are extended as cinnamates or α-methylcinnamates. The cinnamoyloxy derivatives exhibit B_6, B_1, and B_{X5} phases on ascending the homologous series (series **IV**). Interestingly, the compounds exhibiting B_{X5} phase show an antiferroelectric switching behavior.

However, the compounds containing α-methylcinnamoyloxy groups are nonmesomorphic and the melting points and the associated enthalpy values are recorded in Table 7.

F. Comparison Between the Mesophases of Compounds Derived from 1,3-Dihydroxybenzene and 2,7-Dihydroxynaphthalene as the Central Units. It is known from the literature[1,13] that the bent-core compounds derived from resorcinol[1] show a B_2 phase, and the corresponding analogues derived from 4-cyano-resorcinol[13] show direct transitions from calamitic to banana phases. This is due to a fact that the cyano group substitution at position 4 changes the conformation of the arms such that the bending angle would be about $120 < \theta < 150$. Similar observations can be made by replacing a 1,3-phenylene central unit with a 2,7-naphthylene group.

It is very clear from our investigations that the compounds derived from 2,7-dihydroxynaphthalene exhibit a nematic phase irrespective of the position of fluorine in the side wings for both cinnamates and α-methylcinnamates. Interestingly, the nematic phase gets stabilized even for *n*-tetradecyl chains without suppressing the B-phases. However, the corresponding analogues, which are derived from 1,3-dihydroxybenzene, do not show a nematic phase even for shorter chains. In both the central cores one would expect the bending angle of about 120°. This is an indirect evidence that the compounds derived from 2,7-dihydroxynaphthalene as the central unit must be providing a bending
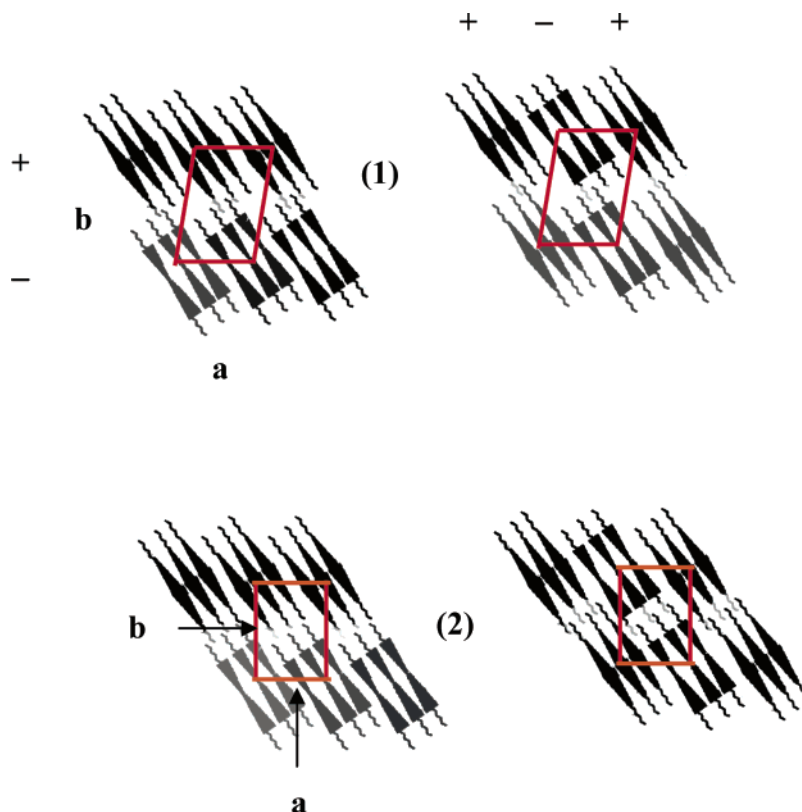
Figure 13. (1) Proposed models for an oblique lattice with an antiferroelectric ordering of the molecules in the adjacent layers or columns (B_{X3} mesophase). Similarly, (2) are the proposed models for a rectangular lattice (B_{X5} mesophase); + and − signs indicate the alternating polarization direction; *a* and *b* are the lattice parameters.
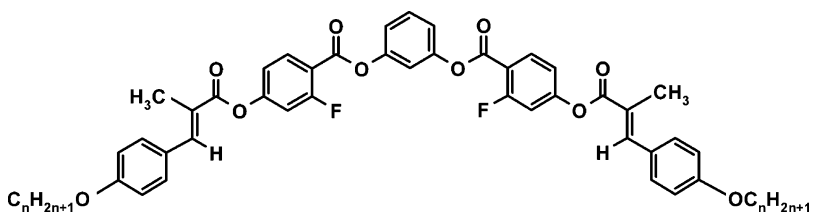
Table 6. Transition Temperatures (T/°C) and Enthalpies (ΔH/kJ mol^{-1}, in Italics) for Compounds of Series IV[a]

compound	n	Cr		B_{X5} (Col$_{rAF}$)		B_1 (Col$_r$)		B_6 (Sm$_{intercal}$)		I
31	6	.	137.5	−		.	141.0	.	143.0[c]	.
			58.5						*12.1*	
32	10	.	111.0	.	(98.5)	−		−		.
			49.9		*10.5*					
33	12	.	110.5	.	(102.0)	−		−		.
			52.2		*11.1*					
34	14	.	114.5	.	(111.0)	−		−		.
			72.3		*15.9*					
35	16	.	113.5	.	119.0	−		−		.
			62.5		*17.8*					
36	18	.	108.0	.	122.0	−		−		.
			127.2		*17.4*					

[c] Enthalpy denoted is the sum of B_6 to I and B_6 to B_1 phase transitions.

angle of about $120 < \theta < 150$, which is attributable to conformational changes in the arms. Hence, direct transitions from calamitic phases to B-phases are feasible. Compounds derived from 1,3-dihydroxybenzene as the central unit provide a bending angle of about 120° and hence only the B-phases are obtained. Since the nematic phase is not observed in the 1,3-dihydroxybenzene derivatives, the induction of a nematic phase is not mainly due to the flexible cinnamates, but due to the bending angle defined by the central core. Interestingly, compounds derived from 2,7-dihydroxynaphtha-lene exhibit an oblique lattice (B_{X3} mesophase) without electrooptical switching. On the contrary, the mesophase of compounds containing 1,3-dihydroxybenzene central core form a rectangular lattice with an antiferro-electric switching behavior. In addition, the compounds containing α-methylcinnamoyloxy groups having 2,7-dihydroxy-naphthalene as the central unit exhibit B-phases and a nematic phase while the corresponding 1,3-dihydroxy-benzene analogues do not show any mesophase despite the fluorine substitution on the middle phenyl ring. From these observations one can infer that 2,7-dihy-

Table 7. Transition Temperatures (*T*/°C) and Enthalpies (Δ*H*/kJ mol⁻¹, in Italics) for Compounds of Series V[a]

compound	*n*	Cr		I
37	8	.	89.0	.
			54.4	
38	16	.	96.5	.
			118.3	

droxynaphthalene is a good angular central unit when compared with 1,3-dihydroxybenzene either to generate or to stabilize the mesophases and also to obtain rich polymorphism.

Conclusions

A few novel series of bent-core compounds containing cinnamoyloxy or α-methylcinnamoyloxy groups in the sidearms have been synthesized, and the mesophases exhibited by them have been compared. The influence of the central angular unit on the occurrence of mesophases has been investigated. The higher homologues of compounds containing cinnamoyloxy groups in the sidearms which are derived from 2,7-dihydroxynaphthalene show a direct transition from nematic phase to a columnar phase with an oblique lattice. The corresponding analogues derived from 1,3-dihydroxybenzene show a rectangular columnar phase which, interestingly, shows an antiferroelectric switching behavior. Compounds derived from a naphthylene central unit containing α-methylcinnamoyloxy group in the sidearms show a direct transition from a nematic phase to an antiferroelectric B₂ phase. The corresponding analogues derived from 1,3-dihydroxybenzene do not show any mesophase. These observations indicate that 2,7-dihydroxynaphthalene is a good central unit to induce banana phases with polymorphism when compared to the corresponding 1,3-dihydroxybenzene derivatives. However, the transition temperatures are higher in the former. A fluorine lateral substituent induces an interesting phase sequence such as direct transition from a nematic phase to an antiferroelectric B₂ phase and to a columnar B₁ phase as well. The orthogonal arrangement of molecules in the B₁ phase was found in two homologous series of compounds containing 2,7-naphthylene central cores.

Experimental Section

Synthesis. The commercially obtained 2,7-dihydroxynaphthalene and 1,3-dihydroxybenzene were purified before use. 4-Benzyloxybenzoic, 2-fluoro-4-benzyloxybenzoic, and 3-fluoro-4-benzyloxybenzoic acids were prepared as reported earlier.[16] The *E*-4-*n*-alkoxycinnamic acids were prepared as described in the literature.[26] The *E*-4-*n*-alkoxy-α-methylcinnamic acids were prepared following a procedure described earlier.[27] The transition temperatures obtained for these intermediate compounds agree well with the reported values.[28]

Supporting Information Available: Figures S1–S6, experimental details, and analytical data for at least one compound of each series (pdf). This material is available free of charge via the Internet at http://pubs.acs.org.

CM0494498

(26) Gray, G. W.; Jones, B. *J. Chem. Soc.* **1954**, 1467.
(27) Johnson, J. R. *Organic Reactions*; Adams, R., Bachmann, W. E., Fieser, L. F., Snyder, J. R., Eds.; John Wiley & Sons: New York, 1942; vol. 1, p 210.
(28) Sadashiva, B. K. *Mol. Cryst. Liq. Cryst.* **1976**, *35*, 205.